Polymer Chemistry

Tuning Dispersity of Linear Polymers and Polymeric Brushes Grown from Nanoparticles by Atom Transfer Radical Polymerization

Journal:	*Polymer Chemistry*
Manuscript ID	PY-MRV-08-2021-001178.R1
Article Type:	Minireview
Date Submitted by the Author:	02-Oct-2021
Complete List of Authors:	Yin, Rongguan; Carnegie Mellon University, Chemistry Wang , Zongyu ; Carnegie Mellon University, Department of Chemistry Bockstaller, Michael; Carnegie Mellon University, Materials Science and Engineering Matyjaszewski, Krzysztof; Carnegie Mellon University, Department of Chemistry

MINIREVIEW

Tuning Dispersity of Linear Polymers and Polymeric Brushes Grown from Nanoparticles by Atom Transfer Radical Polymerization

Received 00th January 20xx,
Accepted 00th January 20xx

DOI: 10.1039/x0xx00000x

Rongguan Yin,[a] Zongyu Wang,[a] Michael R. Bockstaller[b] and Krzysztof Matyjaszewski*[a]

Molecular weight distribution imposes considerable influence on the properties of polymers, making it an important parameter, impacting morphology and structural behavior of polymeric materials. Atom transfer radical polymerization (ATRP) has established itself as a powerful tool to prepare polymers with predetermined molecular weight, preserved chain-end functionality, and low dispersity. More recently, ATRP has also been shown to provide a means to deliberately broaden molecular weight distributions, and, *via* the retaining living chain-ends, to enable the formation of block copolymers with designed block dispersity, featuring new microstructures and potentially attractive properties. Similar methodologies have been developed to facilitate tuning of the dispersity of polymeric brushes grown from nanoparticles thus resulting in hybrid materials with enhanced fracture toughness and high inorganic content. Recent advances have given access to brush architectures comprised of uni- and bimodal block copolymers with unique morphologies along with interesting mechanical, thermal, and optical properties.

1. Introduction

Polymer dispersity (*Đ*), previously termed as "polydispersity index (PDI)" or "molecular weight distribution (MWD)", describes the distribution or heterogeneity of molecular weight of a given (co)polymer. The dispersity index *Đ* is defined as the ratio of weight average molecular weight (M_w) to number average molecular weight (M_n) and thus provides information about the normalized width of the distribution of molecular weight. Generally, *Đ* is greater than 1, except when all polymer chains have identical molecular mass and constitution (i.e. uniform polymer).[1] Whereas in academia, the accomplishment of uniform polymers has long been viewed as the desirable goal,[2-4] there is no "good or bad" when judging narrow and broad MWD. It has been established that distinct physical properties of polymer materials exhibit different and specific dependencies on molecular dispersity. This has set the stage for research in methodologies that facilitate the deliberate tuning of dispersity to enhance specific material properties and enable novel applications.[5-9]

Controlled radical polymerization (CRP), also known as reversible-deactivation radical polymerization (RDRP), enables precise tuning of the compositions and architectures of polymers. This strategy provides good control over the molecular weight, dispersity, and end-group functionality during polymerization.[10-14] There are three most often used CRP techniques, including reversible addition fragmentation chain-transfer (RAFT) polymerization,[15-17] nitroxide-mediated polymerization (NMP),[18-20] and atom transfer radical polymerization (ATRP).[21-23] Research in our group has been focused on developing methods to improve and optimize ATRP conditions, including monomer library expansion,[24, 25] highly active ligands,[26-28] catalyst diversity,[29, 30] numerous external stimuli,[31-34] and oxygen tolerance.[35-37] Nowadays, the advanced ATRP strategies have endowed precise and efficient syntheses of polymers with complex architectures and specific properties.[38, 39]

Polymer-inorganics nanohybrids comprise functional polymers grafted from inorganic nanostructured compounds with well-designed compositions and architectures.[40-42] They have attracted much attention since the nanofillers can enhance the properties of the matrix while preserving the economic formability of polymer host. Moreover, connectivity and interactions between the components can generate synergistic effects and novel properties, making the polymer nanohybrids promising materials available for optical, electrical, mechanical, and biomedical applications.[43-46] The development of polymer nanohybrids mainly relies on two factors: surface modification and surface-initiated polymerization. As for the surface modification, by anchoring functional groups surrounded the nanoparticle substrate with covalent bonds, the anchoring agents enable the nanocores to graft polymers *via* either "grafting-from", "grafting-through", or "grafting-onto" approaches.[40, 47, 48] Considering the polymerization step, our group utilizes surface-initiated atom transfer radical

[a] Department of Chemistry, Carnegie Mellon University, Pittsburgh, Pennsylvania 15213, United States. Email: km3b@andrew.cmu.edu
[b] Department of Materials Science & Engineering, Carnegie Mellon University, Pittsburgh, Pennsylvania 15213, United States.

polymerization (SI-ATRP) to graft diverse functional polymers from nanoparticles, where silane-based ATRP initiators with alkyl bromides are immobilized on particle surface by strong Si-O bonds.[49-51] The molecular weight and dispersity of polymer ligands can be well-controlled through the "living" polymerization process.

In this minireview, we summarize the recent progress in controlling and tuning dispersity of linear polymers and polymeric brushes grown from nanoparticles by ATRP, where morphology and properties of particle brushes with homopolymer tethers, unimodal block copolymer tethers, and even bimodal block copolymer tethers will be highlighted. Compared to linear polymers, when tuning the dispersity, polymer chains grown from nanoparticles give rise to significant variations in the resulting morphology thus endowing unique properties which can potentially be applied as specific functional materials.

2. Dispersity control in CRP

In conventional radical polymerization (RP), a broad MWD (M_w/M_n = 1.5 - 2) is caused by slow initiation and fast termination (*via* combination and/or disproportionation) due to the high activity of radicals.[52] However, in all CRP systems, a dynamic equilibrium between propagating radicals and dormant species is established. The propagating radicals can be rapidly trapped through the activation-deactivation process or by a reversible transfer process. The fast (instantaneous) initiation starts concurrent growth of all chains, meanwhile minimizing the contribution of terminated chains by introducing a large pool of dormant species, thus resulting in polymers with a narrow MWD.[53]

In degenerative transfer (DT) processes or RAFT, dispersity is expressed as Eq. (1):[54]

$$Đ = \frac{M_w}{M_n} = 1 + \frac{1}{DP_n} + \left(\frac{k_p}{k_d}\right)\left(\frac{2}{p} - 1\right) \quad \text{Eq. (1)}$$

Where p represents the conversion of polymerization, k_p/k_d denotes the ratio of rates of propagation and deactivation. In RAFT polymerizations, dispersity can be precisely tuned by mixing chain-transfer agents with different activity.[55, 56] Since the exchange reaction with the transfer agent can also be considered as a deactivation process, it also impacts the overall chain length. Therefore, the MWD should not rely on the degree of polymerization (DP_n) if the concentration of the thermal initiators is relatively small compared to the transfer agent concentration.

The detailed kinetic study of the DT process,[57, 58] demonstrated that dispersity can be calculated through:

$$Đ = \frac{1}{DP_n} + \frac{1}{p}\left[2 + \frac{(2-p)(1-\beta)}{(\beta-\alpha)} - \frac{2\alpha(1-\alpha)}{(\beta^2-\alpha^2)}\frac{1-(1-p)^{1+\beta/\alpha}}{p}\right] \quad \text{Eq. (2)}$$

Where α represents the fraction of active chain ends and β is the ratio of the rate of activity exchange and propagation (i.e., k_{ex}/k_p). For most polymerizations (with DP_n larger than 25) reaching full conversion (p = 1), Eq. (2) can be simplified as:

$$Đ \approx \frac{\beta+1}{\beta+\alpha} \quad \text{Eq. (3)}$$

Which leads to the simplest equation if $\beta \gg \alpha$:

$$Đ \approx 1 + \frac{1}{\beta} = 1 + \frac{k_p}{k_{ex}} \quad \text{Eq. (4)}$$

For the ATRP process, $Đ$ is given as:[53, 59, 60]

$$Đ = \frac{M_w}{M_n} = 1 + \frac{1}{DP_n} + \left(\frac{k_p[R-X]_0}{k_d[Cu^{II}X/L]}\right)\left(\frac{2}{p} - 1\right) \quad \text{Eq. (5)}$$

However, since the radical termination reactions cannot be avoided and can considerably influence the polymerization system, a modified equation for $Đ$ was reported to account for the dead chains:[59, 61]

$$Đ = 1 + \frac{1}{DP_n} + \left(\frac{k_p[R-X]_0}{k_d[Cu^{II}X/L]}\right)\left(\frac{2}{p} - 1\right) + \left(\frac{k_t k_a[Cu^I/L]_0}{4k_p k_d[Cu^{II}X/L]_0}\right)p \quad \text{Eq. (6)}$$

Where k_a and k_t are rate coefficients of activation and termination, respectively. The value of $Đ$ is the result of a balance between the activation/deactivation cycle numbers and the terminated chain fractions.[59] Judging from Eq. (5) where termination is negligible, the dispersity becomes lower with increasing monomer conversion (p) and degree of polymerization (DP_n), showing an inverse relationship with the initial concentration of initiator. It also correlates with the ratio of propagation/deactivation rate (R_p/R_d), where rate of deactivation is determined by the product of the concentration of deactivator ($[Cu^{II}X/L]$, where X and L represent Cl or Br, and multidentate nitrogen-based ligand, respectively) and the rate constant of deactivation. Therefore, good control over MWD in ATRP needs a certain deactivator concentration together with fast initiation to achieve uniform chain growth.[22, 62] Typically, in conventional ATRP (also referred to as traditional or normal ATRP), sufficiently high Cu catalyst concentration is needed to reach high monomer conversion.[21, 63-66] However, a high amount of transition metal complexes may complicate polymers purification.[67] Although various methods have been applied to remove the copper residues,[27, 68-71] the most efficient alternative solution is to diminish the amount of metal catalyst while maintaining a sufficient polymerization rate. If the catalyst concentration is too low, the slow activation (initiation) may cause the MWD broadening:[72]

$$R_a = k_a[Cu^I/L][RX] \quad \text{Eq. (7)}$$

The development of higher activity catalysts (ligands) and new ATRP procedures helped to diminish the amount of Cu to ppm levels through successive regeneration of the deactivator (Figure 1).[23] These methods include activators regenerated by electron transfer (ARGET) ATRP,[73-75] initiators for continuous activator regeneration (ICAR) ATRP,[76-78] supplemental activator and reducing agent (SARA) ATRP,[79-81] and ATRP triggered by external stimuli such as electric current (*e*ATRP),[34, 70, 82] light (photo-ATRP),[32, 83-85] and ultrasonication (sono-ATRP)/mechanical force (mechano-ATRP).[31, 86-88]

Good control over MWD is accessible *via* small quantities of Cu catalysts with highly active ligands providing high values of K_{ATRP} ($K_{ATRP} = k_a/k_d$). Under this condition nearly all of the Cu catalyst is in the X-Cu^{II}/L state.[76] Comparative study was performed using four X-Cu^{II}/L complexes, such as $CuCl_2$/Me_6TREN, $CuCl_2$/TPMA, $CuCl_2$/PMDETA, and $CuCl_2$/dNbpy. ICAR ATRP of styrene (St) and methyl methacrylate (MMA) mediated by $CuCl_2$/Me_6TREN and $CuCl_2$/TPMA exhibited narrow MWD (M_w/M_n < 1.2), while control over polymerizations mediated by $CuCl_2$/PMDETA and $CuCl_2$/dNbpy was relatively poor (M_w/M_n > 1.6). The good agreement between theoretical and experimental molecular weights suggested that the higher dispersity was caused by smaller deactivation rate constants but minimal termination. The latter two catalysts have lower K_{ATRP} values and lower fraction of X-Cu^{II}/L deactivators than the former, which resulted in uneven polymer growth.

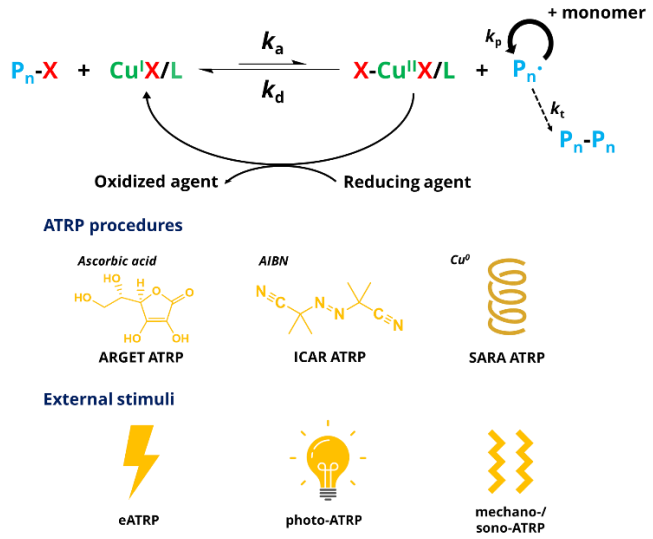

Figure 1. ATRP processes with regeneration of the Cu catalysts used at ppm amounts.

ARGET ATRP employs a low copper concentration in the presence of tin(II) 2-ethylhexanoate ($Sn(EH)_2$) as the reducing agents, which continuously regenerate Cu^{I} (ATRP activator) from Cu^{II} (ATRP deactivator).[73, 74] The excess of reducing agents enables the ATRP to start with oxidatively stable Cu^{II} species and even tolerate a limited amount of oxygen or other radical traps in the system. Such low copper concentration (i.e., only 10 ppm of X-Cu^{II}/L versus monomer) in the polymerization of St still provided polymers with narrow MWD (M_w/M_n = 1.17). While molecular weight was well controlled, when the Cu level was decreased to 1 ppm, a higher $Đ$ =1.64 was observed.

Additionally, increased concentration of halide anions contributes to well-controlled ATRP in aqueous media. Concerning ATRP in water, partial dissociation of halide ions from X-Cu^{II}/L leads to insufficient deactivation rate of the propagating radicals. The Cu^{I}/L as the activator tends to disproportionate or partially dissociate as well, thus resulting in poorly controlled polymerization.[89] Traditional methods of performing ATRP in water require a low ratio of activator/deactivator and overall high concentration of copper to minimize the deactivator dissociation. New methods with excess halide salt improve the regeneration of the deactivator complex to gain control over polymerization, forming polymers with narrow MWD and retention of chain-end functionality. Aqueous ARGET ATRP with excess chloride anions,[90] and ICAR ATRP with excess bromide anions,[91] revealed good control over polymerizations of oligo(ethylene oxide) methyl ether methacrylate (OEOMA) with 100 ppm or even lower level of copper catalyst and showed narrow MWD (M_w/M_n < 1.3). At a too low concentration of salt (< 10 mM), polymers with broader MWD (M_w/M_n = 1.48) were formed due to a dissociation of halide anion in X-Cu^{II}/L.[90]

ARGET ATRP employs an excess of reducing agents to maintain the activator concentration throughout the polymerization. If the initiator is below a critical concentration, the MWD also starts to broaden.[92] For example, the concentration of a small-molecule initiator, ethyl 2-bromoisobutyrate ($[EBiB]_0$) was varied to perform ARGET ATRP of MMA. When $[EBiB]_0$ was larger than 100 ppm (compared to monomer), the kinetic plots exhibited a linear trend, resulting in polymers with low dispersity (M_w/M_n < 1.4). However, when $[EBiB]_0$ was smaller than 100 ppm, conversion stopped at ca. 3h, suggesting all chains were terminated. The presence of large fractions of terminated chains broadened MWD. With the lowest $[EBiB]_0$ (12.5 ppm), the dispersity was 2.11. When $[EBiB]_0$ < $[Cu^{II}X/L]$ < $[Sn(EH)_2]$, Larger fraction of chains can be terminated. However, in polymerization of St, decreasing $[EBiB]_0$ caused a moderate increase in dispersity (M_w/M_n = 1.52), along with a dramatic increase of apparent initiating efficiency to 422% at the lowest $[EBiB]_0$. This can be attributed to the thermal self-initiation (TSI) behavior of St, where chains initiated by the newly formed radicals were introduced into the reaction.[93]

Besides using traditional reducing agents (like L-ascorbic acid[94] and $Sn(EH)_2$[73]), more recently, inorganic sulfites,[95] eutectic Ga–In alloy (EGaIn),[96] and some other external stimuli can also mediate the ATRP process at relatively low Cu catalyst concentration. In ultrasonication-induced ATRP (sono-ATRP), ultrasonic waves propagate through aqueous media and produce hydroxyl radicals, which can react with a vinyl monomer to form carbon based radicals that further reduce Cu^{II} to Cu^{I} and trigger the ATRP.[31] Successful aqueous sono-ATRP was carried out in polymerization of OEOMA and 2-hydroxyethyl acrylate (HEA) with ppm amounts of Cu catalyst, leading to polymers with narrow MWD. Ultrasonic agitation also favored interactions of piezoelectric nanoparticles with Cu catalysts in mechanically controlled ATRP (mechano-ATRP). The mechano-induced electron transfer from the surface of nanoparticles promoted the reduction from Cu^{II} to the activator Cu^{I}/L complex. Related piezoelectric materials include barium titanate ($BaTiO_3$, 4.5 wt%)[87] and a lower loading of zinc oxide (ZnO, 0.6 wt%)[86] nanoparticles. Both systems showed the predetermined molecular weight and narrow MWD. Electrochemically mediated ATRP (*e*ATRP) maintains some advantages of ARGET ATRP such as low concentration of Cu catalyst and tolerance to a limited amount of oxygen.[34] Moreover, *e*ATRP eliminates reducing agents that may not be

environmentally benign and promotes catalyst removal *via* electrodeposition. This happens when a very negative potential is applied and reduction from Cu^{I} to Cu^{0} occurs at the working electrode. Interestingly, applying progressively more negative potential led to a faster polymerization at the expense of polymerization control (M_w/M_n > 1.5).[82] Subsequent optimizations using non-platinum electrodes represent one step further toward scale-up and commercialization of this polymerization technique.[97, 98] In photoinduced ATRP (photo-ATRP) systems, the excitation of Cu^{II} catalysts under UV irradiation is followed by a reductive quenching process with electron donors as the main pathway for generation of Cu^{I} activators, maintaining control over molecular weight and narrow MWD with low concentration of Cu catalyst.[35, 99-101] Since UV light may have low depth of penetration, optimizations of photo-ATRP under visible light are explored to maintain narrow MWD.[83, 102, 103]

3. Tuning dispersity, chain-end functionality, and block copolymer architectures

Tuning dispersity in a broad range becomes advantageous for some material applications, since polymers with either narrow or broad MWD provide materials with specific properties and functions. Several methods for tailoring the dispersity (Figure 2) involve blending pre-synthesized polymers with multiple molecular weights,[104-106] feeding initiators during polymerization *via* a syringe pump,[107, 108] exploiting flow chemistry by adjusting reaction conditions,[109-111] mixing chain-transfer agents in RAFT polymerization,[55, 56] using a temperature-selective iodine-mediated radical copolymerization,[112] termination process[113] *via* radical coupling[114] or *via* addition of capping agents,[115, 116] or varying concentration of deactivators, according to Eq. (5). The dispersity values in ARGET ATRP and photo-ATRP can be further increased by combination of low deactivator concentration and termination to values of 2.30 for polystyrene via phenylhydrazine addition,[117] 2.48 for poly(n-butyl acrylate)[73] and 1.80 for poly(methyl methacrylate).[118]

ATRP is a radical polymerization technique with unavoidable termination of growing chain ends. This contributes to broadening the MWD to a different extent and thus can be used to tune dispersity. This can happen spontaneously or can be forced by addition of termination agents. For example, MWD of poly(*tert*-butyl acrylate) (P*t*BA, M_w/M_n = 1.08 – 1.80) and of polystyrene (PS, M_w/M_n = 1.07 – 2.30) in ATRP were varied by addition of phenylhydrazine.[117] This diminished the attainable conversion and broadened the MWD by reducing the chain-end fidelity, which impeded chain extension in block copolymerization. Phenylhydrazine reacted with the polymeric alkyl halides by nucleophilic substitution leading to chain termination, in addition to acting as a reducing agent.[76] Analogous methodologies of deactivating chain end to broaden the MWD include incorporating nitroxides as radical scavengers[115] or sodium azide (NaN_3) as nucleophiles.[116]

On the other hand, dispersity can be well tuned with retained chain-end fidelity. Using ARGET ATRP, polymerizations with tuneable monomodal MWD (M_w/M_n = 1.1 – 2.0) were developed by adjusting the concentration of the copper catalyst and reaction temperature.[9, 73, 74, 119] Tuning dispersity is also possible for monomers with higher K_{ATRP} such as acrylonitrile.[120, 121] By gradually decreasing the Cu catalyst concentration from 50 to 1 ppm, the M_w/M_n correspondingly increased from 1.21 to 1.41.[122] Despite increased dispersity, chain-end fidelity was preserved and the living features of the macroinitiators were confirmed by chain extension, where MWD of the second block was also tuneable and calculated through Eq. (8) (ω_A and ω_B are the weight fraction of block A and block B, respectively):[123]

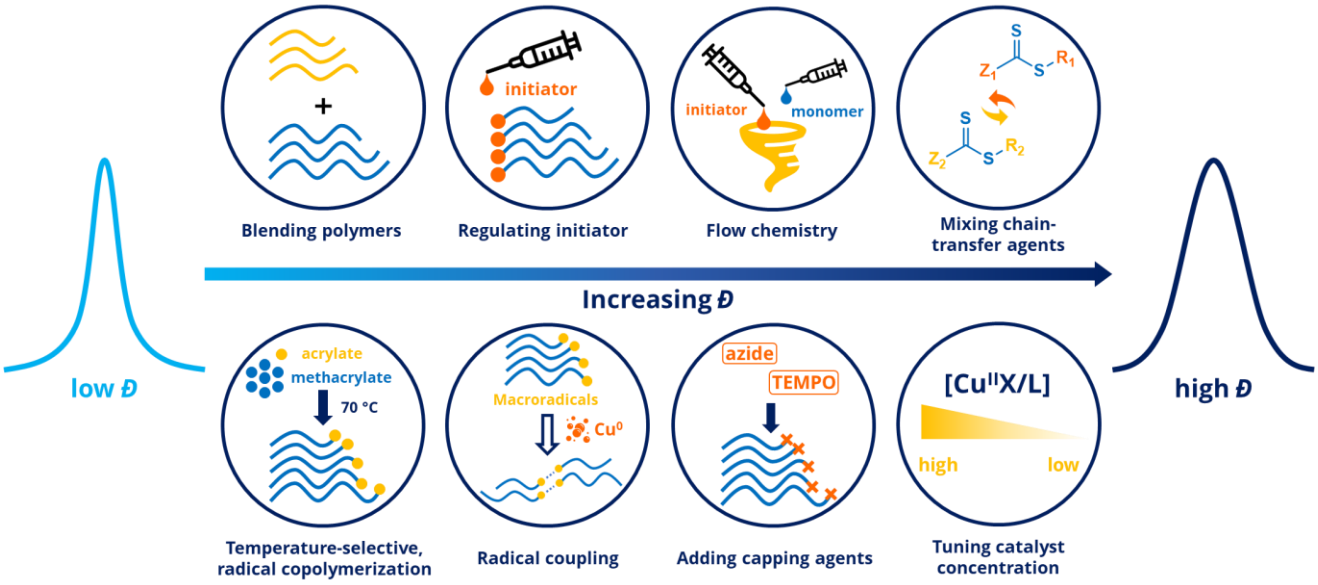

Figure 2. Typical strategies on tailoring the polymer dispersity.

$$Đ_{AB} = \omega_A^2 (Đ_A - 1) + \omega_B^2 (Đ_B - 1) + 1 \quad \text{Eq. (8)}$$

Recently, in a similar way, by decreasing the concentration of copper catalyst, a gradual broadening of monomodal and almost symmetrical molecular weight distributions (M_w/M_n = 1.05 – 1.75) with approximately constant M_n was demonstrated using photo-ATRP.[124] This approach was extended to iron-catalyzed photo-ATRP (M_w/M_n = 1.18 – 1.80) by varying the concentration of $FeBr_3$/TBABr catalyst.[118] High end-group functionality was maintained in both cases as confirmed by the subsequent chain extension to form block copolymers. Moreover, the final dispersity of a diblock could be fine-tuned based on a "broad" first block while keeping the monomodal shape of MWD, illustrated by "broad to narrow", "broad to medium", and "broad to broad" transitions (Figure 3). Polymers with broad MWD also retained the terminal functionality, which seems contrary to a typical belief that broad distribution results from termination. Using 7 ppm or lower concentration of Cu catalyst, the polymerization ceased at approximately 48% conversion, together with broad MWD and a deviation between theoretical M_n and the M_n measured by size exclusion chromatography (SEC).[125] The latter was ascribed to large amounts of unreacted initiators.

Synthesis of block copolymers (BCP) *via* anionic polymerization,[126] became a fundamental field in polymer chemistry. Apart from properties contributed from each block, BCP undergo microphase separation to form nanostructured materials if the blocks are incompatible.[127] MWD breadth in BCP was proposed to cause increased compositional fluctuations,[128] which was later confirmed by self-consistent-field simulations, suggesting BCP with mono- and polydisperse blocks tend to stabilize topological defects and shift the stability regions of various morphologies.[129, 130]

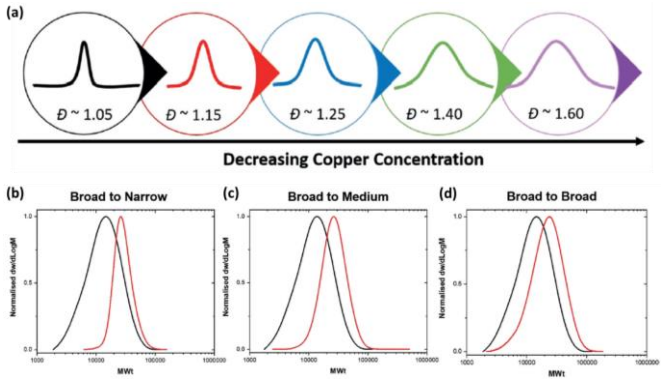

Figure 3. (a) SEC analysis of the polymerization of MA, illustrating increasing near-symmetrical dispersity as catalyst concentration is lowered. (b-d) Chain extensions from a high-dispersity PMA macroinitiator (*Đ* =1.57) yielding P(MA-b-MA) with a range of final dispersity b) *Đ* =1.14 c) *Đ* =1.28, and d) *Đ* =1.47 utilizing photoinduced ATRP, reprinted from ref.124 with permission from John Wiley and Sons, copyright 2019.

Chain-end fidelity was well preserved with tuneable dispersity by varying Cu catalyst concentration in ARGET ATRP, enabling BCP synthesis with near-symmetric block-selective MWD. Based on this strategy, poly (St-block-MA) (PS-*b*-PMA) copolymer with narrow MWD PS block (M_w/M_n = 1.11) and broad MWD PMA block (M_w/M_n = 1.77) was prepared (i.e. $(PS\text{-}PMA)_{narrow\text{-}broad}$). This copolymer self-assembled into a hexagonally perforated lamellar (HPL) morphology which was stable under prolonged thermal annealing and hence interpreted to be an "equilibrium morphology" (Figure 4).[9] Since HPL morphology was considered to be metastable in diblock copolymers, the stabilization of the HPL morphology suggested that the skewness of MWD in BCP is a significant parameter for the structure selection amid the microphase separation process. This indicated the relevance of manipulating both the breadth and the symmetry of MWD toward the tailored synthesis of nonregular microstructures in BCP. A subsequent analysis focused on the effect of homopolymer addition on structure hierarchy in lamellar amorphous PS-PMA BCPs with block-selective dispersity (i.e., a narrow-MWD PS and broad-MWD PMA block).[131] While incorporating PMA homopolymer into the broad-MWD PMA domain could induce structural variations, the addition of PS homopolymer to the narrow-MWD PS domain induced a more noticeable expansion of lamellar domains attributed to the segregation of homopolymers into the center region of the narrow-MWD domain in BCP. Additionally, as the added PS homopolymer concentration increased, the constitution of a stabilized bicontinuous regime with coexisting lamellar/gyroid microphases was observed. The bicontinuous regime was constrained by uniform lamellar phase regimes within the narrow MWD block domain. BCP/homopolymer blends based on BCP with broad MWD of selective block indicated that MWD is an important parameter and can be efficiently utilized in BCP engineering.

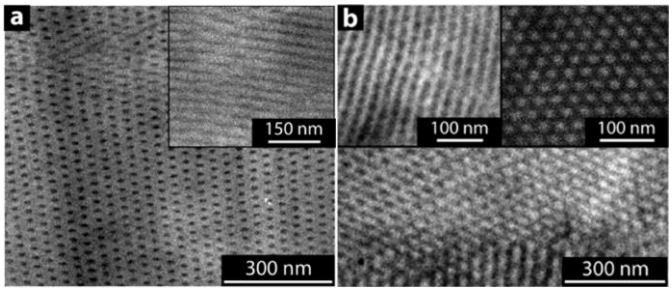

Figure 4. Bright field electron micrographs of PS-PMA samples with similar composition but distinct block dispersity after 72 h of thermal annealing at T = 120 °C and staining with RuO_4 (PMA is dark domain). (a) $(PS\text{-}PMA)_{narrow\text{-}narrow}$: revealing cylindrical microstructure imaged along [001] direction. Inset depicts view along [100] direction. (b) $(PS\text{-}PMA)_{narrow\text{-}broad}$: revealing HPL ($R\bar{3}m$) microstructure imaged at low magnification. The inset on the left depicts the PS-perforations within the PMA layers. The inset on the right shows a plane view revealing the hexagonal arrangement of the PS perforations, reprinted from ref. 9 with permission, copyright 2008 American Chemical Society.

4. Dispersity effects in particle brushes

The conformation and properties of polymeric brushes grown from nanoparticles can be significantly influenced by the uniformity of grafted polymer chains.[132] Broader MWDs of polymeric brushes assist in stabilizing dispersions, even when the average molecular weight of tethered brush is less than that of the matrix.[133] Dispersity may also impact the adhesion of nanoparticles *via* enhancing interparticle entanglement.[133, 134] Accordingly, particle brushes with a tuneable MWD might enable new applications, such as antifouling,[135] mechanical reinforcement,[136] and sensing.[137] Dispersity of particle brushes prepared by SI-ATRP with the same tetherable initiator[48] could be adjusted by using reducing agents and also electrical current[138] or light,[139] similar as in homopolymer systems.

The most accessible method of tuning the MWD of polymeric brushes from nanoparticles by ATRP is adjusting the initial Cu catalyst concentration. With a fixed concentration of surface-modified silica nanoparticles (SiO_2-Br) as initiators but with variable catalyst concentrations, PMMA brushes were grafted from the silica surface with tuneable grafting density and dispersity ($1.16 < M_w/M_n < 2.15$) (Figure 5).[140] Interestingly, 10 ppm Cu acted as a threshold concentration, above which the initiation efficiency (indicated by grafting density) was relatively constant with narrow MWD. However, below the 10 ppm concentration level, the grafting density underwent a significant decrease, concurrent with broadened MWD. This was attributed to slow deactivation, similar to analogous results of tuning dispersity of linear PMMA.

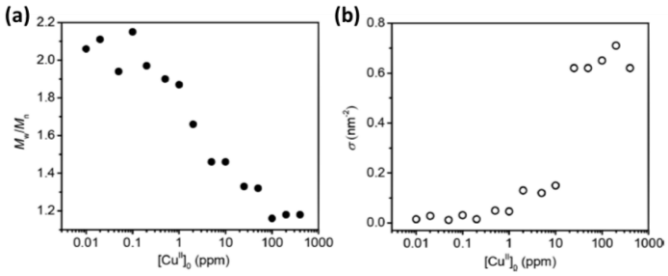

Figure 5. Results of the synthesis of SiO_2-*g*-PMMA particle brushes by ARGET ATRP with different $[Cu^{II}]_0$ (a) dispersity (M_w/M_n) vs $[Cu^{II}]_0$, (b) grafting density (σ) vs $[Cu^{II}]_0$, reprinted from ref. 140 with permission, copyright 2019 American Chemical Society.

The concentration of mild reducing agents had smaller effect on dispersity of particle brushes than the concentration of SiO_2-Br ($[SiO_2\text{-Br}]_0$) (Figure 6).[92] For PS grafted silica nanoparticles with constant Cu catalyst level, dispersity increased from M_w/M_n = 1.19 to 1.92 with decreasing [SiO_2-Br], together with diminishing grafting density, indicating lower initiation efficiency. Meanwhile, for PMMA-grafted silica nanoparticles, as [SiO_2-Br] decreased, relatively narrow MWD remained unaffected. The discrepancy in MWD variations could be attributed to a higher tendency toward combination than disproportionation for PS and the TSI behavior. The latter generated homopolymer impurities preventing good control in PS grafted particle brush materials.

While diminishing the concentration of EBiB initiator led to higher dispersity of PMMA homopolymers, altering the [SiO_2-Br] did not affect the MWD of PMMA brushes grown from nanoparticles. This difference between homopolymers and particle brushes could originate from decreased probability of termination *via* inter-particle coupling, due to localization of initiation sites on the nanoparticle surface. Possibility of radical collisions in a low [SiO_2-Br] system was efficiently reduced compared with low MW initiator molecules. This concept was applied to synthesis of ultra-high molecular weight systems, densely grafted PMMA particle brushes ($M_n > 10^6$) with narrow MWD and without particle brush agglomeration.[141]

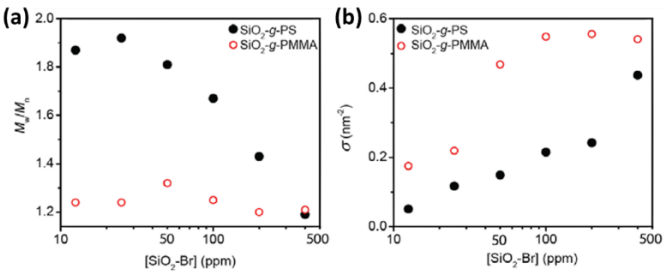

Figure 6. Polymerization of St and MMA on SiO_2–Br nanoparticles by SI-ATRP at different $[SiO_2\text{–Br}]_0$. (a) MWD vs $[SiO_2\text{–Br}]_0$, and (b) plot of grafting density vs $[SiO_2\text{–Br}]_0$, reprinted from ref. 92 with permission, copyright 2019 American Chemical Society.

5. Morphologies and applications

The thermal, mechanical, and rheological properties of polymeric materials rely not only on chemical structure and molecular weight but also on MWD.[8, 142] Despite preference in achieving chain uniformity by most researchers, polymers with either narrow or broad MWD have their own merits regarding mechanical and thermal properties. Polymers with broader MWD bring mechanical enhancement including high modulus, impact strength, and elongation at break, along with a potentially lower glass transition temperature.[6] For example, PS with narrow and broad MWD, (the latter had M_w/M_n = 3.2) was prepared by manually blending low dispersity homopolymers.[143] The high dispersity blends showed a broader relaxation spectrum, lower zero-shear-rate viscosity, larger extensional viscosity, and more noticeable strain hardening behavior. On the other hand, the symmetry of MWD has considerable impact on the physical properties of polymer materials.[108] For example, it was reported that when the MWD skewed towards a higher molecular weight range, the glass transition temperature increased, together with increasing stiffness, thermal stability, and viscosity.[144]

Symmetrical distributions but with tuneable breath stabilized hexagonally perforated lamellar morphology in PS-PMA BCP which could be of interest for applications in separation.[9] Addition of PS homopolymer to a narrow-PS/broad-PMA BCP induced a bicontinuous regime with coexisting lamellar/gyroid microphase.[131] This confirmed the effect of broadness and skewness of MWD for BCP morphology engineering.[5, 7, 8, 145] More recently, the opportunities of harnessing dispersity to enhance the structure and properties of brush particle-based hybrid materials have been realized.

Hence, the effect of dispersity on the mechanical properties and assembly of particle brush systems will be discussed next. This will include homopolymer particle brushes, unimodal block copolymer particle brushes as well as bimodal particle brushes.

When tuning the MWD by changing the Cu catalyst concentration of PMMA grafted particle brushes, transmission electron microscopy (TEM) images revealed the changing particle brushes morphologies (Figure 7).[140] Above 10 ppm Cu, a relatively low dispersity of tethered polymers with a high grafting density was achieved, contributing to evenly distributed particle brushes with isotropic and uniform structures. However, as the Cu catalyst concentration was decreased below 10 ppm, the grafting density decreased and MWD became broader. This resulted in self-assembled anisotropic string-like structures driven by the attraction between patches of bare nanoparticle surfaces.

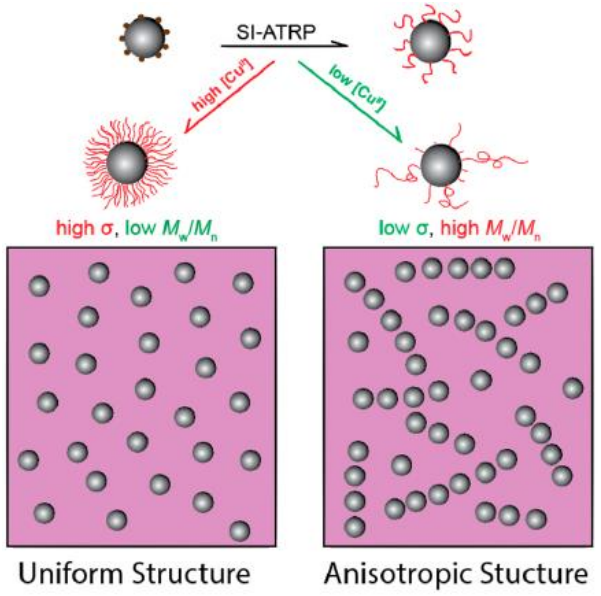

Figure 7. Synthesis of PMMA grafted silica particle brushes with different initial catalyst concentrations and TEM images of monolayer films of particle brushes with different DP and grafting densities. (a) DP = 600, M_w/M_n = 1.16, σ = 0.65 nm^{-2}, (b) DP = 787, M_w/M_n = 1.46, σ = 0.15 nm^{-2}, (c) DP = 2471, M_w/M_n = 1.90, σ = 0.049 nm^{-2}, (d) DP = 1972, M_w/M_n = 2.06, σ = 0.015 nm^{-2}. Red lines highlight the string structures in (c) and (d) insets. Scale bar: 100 nm, reprinted from ref. 140 with permission, copyright 2019 American Chemical Society.

Grafting BCPs from nanoparticles opens avenues for additional morphological control, since nanoparticles can mediate the interactions between BCP constituents. This provides possibility of topological tuning, along with thermal or mechanical effects.[146, 147] In poly(n-butyl acrylate) (PBA)-*b*-PMMA BCP particle brushes synthesized by ATRP, highly segregated and disordered structures were reported.[148] The worm-like cylinders observed by TEM consisted of a string of approximately 3 to 5 silica nanoparticles as the cylinder core (Figure 8).

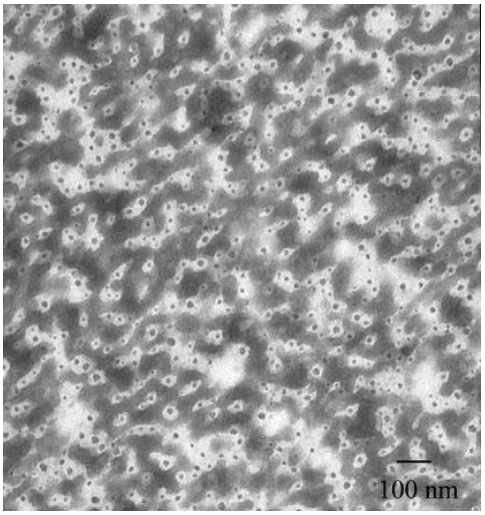

Figure 8. TEM images showing the morphology of the SiO_2-*g*-(PBA-b-PMMA) hybrid nanocomposite, with selective staining of individual blocks. The thin microtomed section was stained with PTA solution, which selectively stains the outer PMMA block. The stained regions are observed as darker regions and the unstained regions are observed as lighter regions, reprinted from ref. 148 with permission, copyright 2018 Elsevier.

The tethering of nanoparticles with bimodal polymer grafts, which can mitigate the constraints of dense unimodal particle brush materials, emerged as a fascinating strategy to integrate the synergistic benefits of both dense and sparse polymeric brushes.[149] The intriguing properties of bimodal MWD particle brush systems came from the complementarity where densely grafted, low molecular weight polymer ligands prevented particle core aggregation, while sparsely grafted, high molecular weight tethers supplied sufficient entanglement, improving the overall mechanical characteristics and processability. The 4-butoxy TEMPO was utilized to partially deactivate Br chain ends for further bimodal MWD particle brush synthesis.[115] TEM images revealed that bimodal MWD samples were uniformly distributed and looked similar to unimodal counterparts due to dense and uniform low molecular weight graft layer (Figure 9).

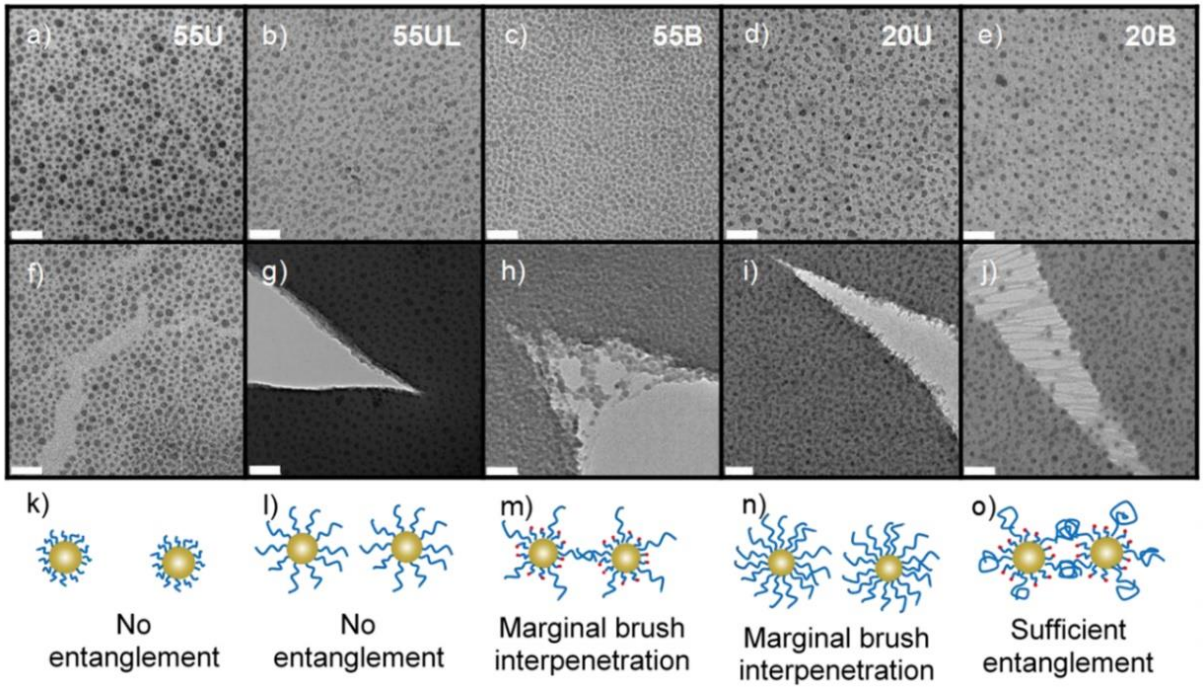

Figure 9. Bright field TEM images of approximate monolayers (a–e), crack formation (f–j), and illustrations of cracks (k–o) of the five samples. Unimodal sample 55U (SiO_2-*g*-PS_{80}, a, f, k): extensive crack propagation. Unimodal sample 55UL (SiO_2-*g*-PS_{170}, b, g, l): sharp crack formation. Bimodal sample 55B (SiO_2-*g*-*bi*-$PS_{13,170}$, c, h, m): plastic deformation. Unimodal sample 20U (SiO_2-*g*-PS_{250}, d, i, n): stent-like undulation formation. Bimodal sample 20B (SiO_2-*g*-*bi*-$PS_{69,790}$, e, j, o): craze formation. All scale bars: 100 nm, reprinted from ref. 115 with permission, copyright 2015 American Chemical Society.

However, upon cracking, bimodal MWD samples demonstrated clear crazing. Long grafts with higher molecular weight significantly exceeded the critical segment length for entanglements. However, unimodal grafts showed sharp cracks indicating brittleness and lack of chain entanglement. Mechanical properties of bimodal systems tested by nanoindentation illustrated remarkable improvement in fracture toughness, which even outperformed high molecular weight and densely grafted unimodal particle brushes. Such improvement came from decreased steric constraints on long polymer grafts that promoted entanglements and chain relaxation.

Bimodal BCP particle brushes with tuneable assembly were synthesized using nanoparticles with different grafting densities. The primary PMMA graft layer was extended with PS as the second block (Figure 10).[150] The blocking efficiency and MWD were additionally controlled by the concentration of Cu catalyst. At low extension efficiency (~7%), the observed phase-separated structure was ascribed to the separation of PMMA- and PMMA-*b*-PS- grafted brush type. As the fraction of PS block increased, the microstructures became more uniform as anisotropic strings. Additionally, three different bimodal BCP particle brushes with the first PMMA block possessing high, medium, and low grafting densities were prepared. They showed overall uniform but partially string-like features, connected rings, and continuous cluster network morphologies after PS-graft chain extension, respectively. This provides a new path toward designing hierarchically ordered quasi-one-component materials.

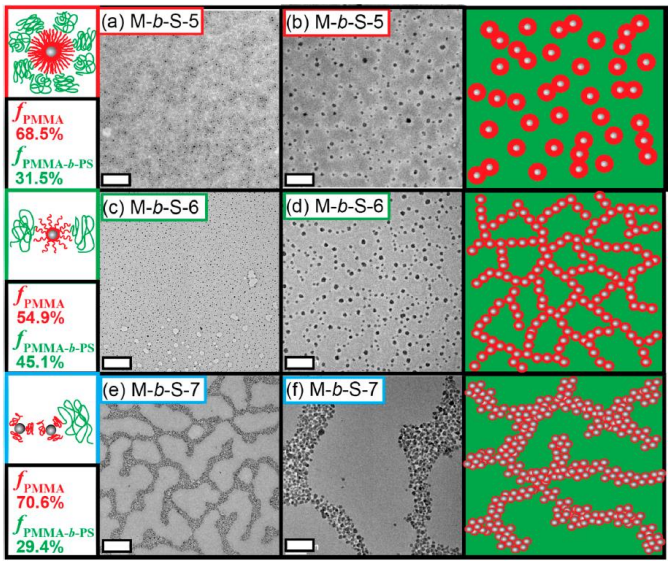

Figure 10. TEM images of bimodal SiO_2-*g*-PMMA-*b*-PS particle brushes. (a, b) densely grafted, (c, d) mediumly grafted, (e, f) sparsely grafted. Scale bar: (a), (c), (e), 500 nm; (b), (d), (f), 100 nm, reprinted from ref. 150 with permission, copyright 2020 American Chemical Society.

Conclusions

Polymers with either narrow or broad, but controlled, molecular weight distribution were successfully prepared by ATRP. Synthesis of polymers with very low dispersity requires

fast initiation, low contribution of chain breaking reactions and fast exchange between active and dormant species. The latter is controlled by the ratio of the rates of deactivation to propagation, i.e., also by the concentration of Cu catalyst. Fast deactivation requires high deactivation rate constants ($k_d > 10^7$ M^{-1} s^{-1}) and a sufficient concentration of deactivator [X-Cu^{II}/L]. Thus, the simplest way to enhance dispersity without sacrificing control of molecular weight and chain end functionality is to decrease concentration of deactivator, typically below 10 ppm vs. monomer; this further depends on the targeted DP. The actual concentration of deactivator depends on the ATRP equilibrium constant (ligand, halogen, medium, temperature), on the halide anion concentration (especially in aqueous systems) and on the rate of activator regeneration (light, electrical current, reducing agents and their feeding rates). Additionally, dispersity and shape of MWD can be affected by slow initiation (feeding, chemical structure, mixture of mono and multifunctional species, etc.) and chain breaking reactions: spontaneous, catalyzed or forced termination, as well as transfer processes. These approaches were applied to synthesis of linear or branched homopolymers, block copolymers, as well hybrid materials. The latter were prepared by grafting from surfaces of inorganic materials modified with anchored ATRP initiators,[40] but also from modified biomolecules (proteins, nucleic acids and carbohydrates).[151] MWD affects many properties and morphological features, and self-assembly of the linear (co)polymers and hybrid materials. Some examples of self-assembly of block copolymers with narrow and broad MWD to form unusual nanostructured morphologies were discussed. They comprised hybrid materials with different grafting density and dispersity, including those with bimodal MWD to generate hierarchically ordered structures.

Though much progress has been made on tuning the average value of dispersity, less research has been focused on the symmetry and skewness of MWD.[152] The latter two variables, depicting the shape of MWD, affect the domain spacing in block copolymers, without significantly changing the overall chemical composition of the final polymer. Further research on symmetry of MWD is needed to investigate its effect on polymer physical properties. We expect that the new ATRP techniques will offer more control of MWD with tailored width and shape, and provide materials with unique physical properties for promising applications in various areas of materials science.

Conflicts of interest

There are no conflicts to declare.

Acknowledgments

Financial support for research on nanoparticle synthesis and mechanical characterization by the National Science Foundation (DMR 1501324 and CMMI-1663305) and for research on structural characterization by the U.S. Department of Energy, Office of Basic Energy Sciences (DE-SC0018784) is gratefully acknowledged.

References

1. A. D. Jenkins, P. Kratochvíl, R. F. T. Stepto and U. W. Suter, *Pure and Applied Chemistry*, 1996, **68**, 2287-2311.
2. B. S. Lele, H. Murata, K. Matyjaszewski and A. J. Russell, *Biomacromolecules*, 2005, **6**, 3380-3387.
3. J. Lawrence, S.-H. Lee, A. Abdilla, M. D. Nothling, J. M. Ren, A. S. Knight, C. Fleischmann, Y. Li, A. S. Abrams, B. V. K. J. Schmidt, M. C. Hawker, L. A. Connal, A. J. McGrath, P. G. Clark, W. R. Gutekunst and C. J. Hawker, *Journal of the American Chemical Society*, 2016, **138**, 6306-6310.
4. J. De Neve, J. J. Haven, L. Maes and T. Junkers, *Polymer Chemistry*, 2018, **9**, 4692-4705.
5. K. E. B. Doncom, L. D. Blackman, D. B. Wright, M. I. Gibson and R. K. O'Reilly, *Chemical Society Reviews*, 2017, **46**, 4119-4134.
6. R. W. Nunes, J. R. Martin and J. F. Johnson, *Polymer Engineering & Science*, 1982, **22**, 205-228.
7. N. A. Lynd, A. J. Meuler and M. A. Hillmyer, *Progress in Polymer Science*, 2008, **33**, 875-893.
8. R. Whitfield, N. P. Truong, D. Messmer, K. Parkatzidis, M. Rolland and A. Anastasaki, *Chemical Science*, 2019, **10**, 8724-8734.
9. J. Listak, W. Jakubowski, L. Mueller, A. Plichta, K. Matyjaszewski and M. R. Bockstaller, *Macromolecules*, 2008, **41**, 5919-5927.
10. K. Matyjaszewski, S. Gaynor, D. Greszta, D. Mardare and T. Shigemoto, *Journal of Physical Organic Chemistry*, 1995, **8**, 306-315.
11. M. Destarac, *Macromolecular Reaction Engineering*, 2010, **4**, 165-179.
12. D. A. Shipp, *Polymer Reviews*, 2011, **51**, 99-103.
13. K. Parkatzidis, H. S. Wang, N. P. Truong and A. Anastasaki, *Chem*, 2020, **6**, 1575-1588.
14. N. Corrigan, K. Jung, G. Moad, C. J. Hawker, K. Matyjaszewski and C. Boyer, *Progress in Polymer Science*, 2020, **111**, 101311.
15. J. Chiefari, Y. K. Chong, F. Ercole, J. Krstina, J. Jeffery, T. P. T. Le, R. T. A. Mayadunne, G. F. Meijs, C. L. Moad, G. Moad, E. Rizzardo and S. H. Thang, *Macromolecules*, 1998, **31**, 5559-5562.
16. L. Barner, T. P. Davis, M. H. Stenzel and C. Barner-Kowollik, *Macromolecular Rapid Communications*, 2007, **28**, 539-559.
17. S. Perrier, P. Takolpuckdee and C. A. Mars, *Macromolecules*, 2005, **38**, 2033-2036.
18. R. B. Grubbs, *Polymer Reviews*, 2011, **51**, 104-137.
19. C. J. Hawker, A. W. Bosman and E. Harth, *Chemical Reviews*, 2001, **101**, 3661-3688.
20. J. Nicolas, Y. Guillaneuf, C. Lefay, D. Bertin, D. Gigmes and B. Charleux, *Progress in Polymer Science*, 2013, **38**, 63-235.
21. J.-S. Wang and K. Matyjaszewski, *Journal of the American Chemical Society*, 1995, **117**, 5614-5615.
22. K. Matyjaszewski and J. Xia, *Chemical Reviews*, 2001, **101**, 2921-2990.
23. K. Matyjaszewski, *Macromolecules*, 2012, **45**, 4015-4039.
24. S. Dadashi-Silab and K. Matyjaszewski, *ACS Macro Letters*, 2019, **8**, 1110-1114.
25. M. Fantin, A. A. Isse, A. Venzo, A. Gennaro and K. Matyjaszewski, *Journal of the American Chemical Society*, 2016, **138**, 7216-7219.
26. A. E. Enciso, F. Lorandi, A. Mehmood, M. Fantin, G. Szczepaniak, B. G. Janesko and K. Matyjaszewski, *Angewandte Chemie International Edition*, 2020, **59**, 14910-14920.

27. G. Szczepaniak, J. Piątkowski, W. Nogaś, F. Lorandi, S. S. Yerneni, M. Fantin, A. Ruszczyńska, A. E. Enciso, E. Bulska, K. Grela and K. Matyjaszewski, *Chemical Science*, 2020, **11**, 4251-4262.
28. T. G. Ribelli, F. Lorandi, M. Fantin and K. Matyjaszewski, *Macromolecular Rapid Communications*, 2019, **40**, 1800616.
29. S. Dadashi-Silab, X. Pan and K. Matyjaszewski, *Macromolecules*, 2017, **50**, 7967-7977.
30. S. Dadashi-Silab, X. Pan and K. Matyjaszewski, *Chemistry – A European Journal*, 2017, **23**, 5972-5977.
31. Z. Wang, Z. Wang, X. Pan, L. Fu, S. Lathwal, M. Olszewski, J. Yan, A. E. Enciso, Z. Wang, H. Xia and K. Matyjaszewski, *ACS Macro Letters*, 2018, **7**, 275-280.
32. X. Pan, N. Malhotra, A. Simakova, Z. Wang, D. Konkolewicz and K. Matyjaszewski, *Journal of the American Chemical Society*, 2015, **137**, 15430-15433.
33. X. Pan, M. Fantin, F. Yuan and K. Matyjaszewski, *Chemical Society Reviews*, 2018, **47**, 5457-5490.
34. A. J. Magenau, N. C. Strandwitz, A. Gennaro and K. Matyjaszewski, *Science*, 2011, **332**, 81-84.
35. G. Szczepaniak, M. Łagodzińska, S. Dadashi-Silab, A. Gorczyński and K. Matyjaszewski, *Chemical Science*, 2020, **11**, 8809-8816.
36. A. E. Enciso, L. Fu, A. J. Russell and K. Matyjaszewski, *Angewandte Chemie International Edition*, 2018, **57**, 933-936.
37. G. Szczepaniak, L. Fu, H. Jafari, K. Kapil and K. Matyjaszewski, *Accounts of Chemical Research*, 2021, **54**, 1779-1790.
38. K. Matyjaszewski, *Advanced Materials*, 2018, **30**, 1706441.
39. K. Matyjaszewski and N. V. Tsarevsky, *J. Am. Chem. Soc.*, 2014, **136**, 6513-6533.
40. J. Yan, M. R. Bockstaller and K. Matyjaszewski, *Progress in Polymer Science*, 2020, **100**, 101180.
41. C. M. Hui, J. Pietrasik, M. Schmitt, C. Mahoney, J. Choi, M. R. Bockstaller and K. Matyjaszewski, *Chemistry of Materials*, 2014, **26**, 745-762.
42. J. Sun, Q. Ma, D. Xue, W. Shan, R. Liu, B. Dong, J. Zhang, Z. Wang and B. Shao, *TrAC Trends in Analytical Chemistry*, 2021, **140**, 116273.
43. M. Zorn, W. K. Bae, J. Kwak, H. Lee, C. Lee, R. Zentel and K. Char, *ACS Nano*, 2009, **3**, 1063-1068.
44. S. Li, T. Liu, J. Yan, J. Flum, H. Wang, F. Lorandi, Z. Wang, L. Fu, L. Hu, Y. Zhao, R. Yuan, M. Sun, J. F. Whitacre and K. Matyjaszewski, *Nano Energy*, 2020, **76**, 105046.
45. R. A. E. Wright, K. Wang, J. Qu and B. Zhao, *Angewandte Chemie International Edition*, 2016, **55**, 8656-8660.
46. P. Pageni, P. Yang, Y. P. Chen, Y. Huang, M. Bam, T. Zhu, M. Nagarkatti, B. C. Benicewicz, A. W. Decho and C. Tang, *Biomacromolecules*, 2018, **19**, 417-425.
47. J. H. Ryu, P. B. Messersmith and H. Lee, *ACS Applied Materials & Interfaces*, 2018, **10**, 7523-7540.
48. J. Yan, X. Pan, Z. Wang, Z. Lu, Y. Wang, L. Liu, J. Zhang, C. Ho, M. R. Bockstaller and K. Matyjaszewski, *Chemistry of Materials*, 2017, **29**, 4963-4969.
49. J. Yan, X. Pan, Z. Wang, J. Zhang and K. Matyjaszewski, *Macromolecules*, 2016, **49**, 9283-9286.
50. J. Pyun and K. Matyjaszewski, *Chemistry of Materials*, 2001, **13**, 3436-3448.
51. J. Pyun, S. Jia, T. Kowalewski, G. D. Patterson and K. Matyjaszewski, *Macromolecules*, 2003, **36**, 5094-5104.
52. K. Matyjaszewski, *Handbook of Radical Polymerization*, 2002, DOI: https://doi.org/10.1002/0471220450.ch8, 361-406.
53. W. A. Braunecker and K. Matyjaszewski, *Progress in Polymer Science*, 2007, **32**, 93-146.
54. K. Matyjaszewski, in *Controlled/Living Radical Polymerization*, American Chemical Society, 2000, vol. 768, ch. 1, pp. 2-26.
55. R. Whitfield, K. Parkatzidis, N. P. Truong, T. Junkers and A. Anastasaki, *Chem*, 2020, **6**, 1340-1352.
56. K. Parkatzidis, N. P. Truong, M. N. Antonopoulou, R. Whitfield, D. Konkolewicz and A. Anastasaki, *Polymer Chemistry*, 2020, **11**, 4968-4972.
57. A. H. E. Mueller, R. Zhuang, D. Yan and G. Litvinenko, *Macromolecules*, 1995, **28**, 4326-4333.
58. A. H. E. Mueller, D. Yan, G. Litvinenko, R. Zhuang and H. Dong, *Macromolecules*, 1995, **28**, 7335-7338.
59. P. Krys and K. Matyjaszewski, *European Polymer Journal*, 2017, **89**, 482-523.
60. F. Lorandi and K. Matyjaszewski, *Israel Journal of Chemistry*, 2020, **60**, 108-123.
61. E. Mastan and S. Zhu, *Macromolecules*, 2015, **48**, 6440-6449.
62. W. Tang and K. Matyjaszewski, *Macromolecular Theory and Simulations*, 2008, **17**, 359-375.
63. J.-S. Wang and K. Matyjaszewski, *Macromolecules*, 1995, **28**, 7901-7910.
64. E. Patten Timothy, J. Xia, T. Abernathy and K. Matyjaszewski, *Science*, 1996, **272**, 866-868.
65. K. Matyjaszewski, T. E. Patten and J. Xia, *Journal of the American Chemical Society*, 1997, **119**, 674-680.
66. R. Whitfield, K. Parkatzidis, K. G. E. Bradford, N. P. Truong, D. Konkolewicz and A. Anastasaki, *Macromolecules*, 2021, **54**, 3075-3083.
67. Y. Shen, H. Tang and S. Ding, *Progress in Polymer Science*, 2004, **29**, 1053-1078.
68. S. C. Hong and K. Matyjaszewski, *Macromolecules*, 2002, **35**, 7592-7605.
69. T. Sarbu and K. Matyjaszewski, *Macromolecular Chemistry and Physics*, 2001, **202**, 3379-3391.
70. P. Chmielarz, M. Fantin, S. Park, A. A. Isse, A. Gennaro, A. J. D. Magenau, A. Sobkowiak and K. Matyjaszewski, *Progress in Polymer Science*, 2017, **69**, 47-78.
71. L. Mueller and K. Matyjaszewski, *Macromol. React. Eng.*, 2010, **4**, 180-185.
72. P. Krys, T. G. Ribelli, K. Matyjaszewski and A. Gennaro, *Macromolecules*, 2016, **49**, 2467-2476.
73. W. Jakubowski and K. Matyjaszewski, *Angewandte Chemie International Edition*, 2006, **45**, 4482-4486.
74. W. Jakubowski, K. Min and K. Matyjaszewski, *Macromolecules*, 2006, **39**, 39-45.
75. Z. Wang, T. Liu, Y. Zhao, J. Lee, Q. Wei, J. Yan, S. Li, M. Olszewski, R. Yin, Y. Zhai, M. R. Bockstaller and K. Matyjaszewski, *Macromolecules*, 2019, **52**, 9466-9475.
76. K. Matyjaszewski, W. Jakubowski, K. Min, W. Tang, J. Huang, W. A. Braunecker and N. V. Tsarevsky, *Proceedings of the National Academy of Sciences*, 2006, **103**, 15309.
77. G. Wang, M. Schmitt, Z. Wang, B. Lee, X. Pan, L. Fu, J. Yan, S. Li, G. Xie, M. R. Bockstaller and K. Matyjaszewski, *Macromolecules*, 2016, **49**, 8605-8615.
78. L. Mueller, W. Jakubowski, W. Tang and K. Matyjaszewski, *Macromolecules*, 2007, **40**, 6464-6472.
79. Y. Zhang, Y. Wang and K. Matyjaszewski, *Macromolecules*, 2011, **44**, 683-685.
80. D. Konkolewicz, Y. Wang, M. Zhong, P. Krys, A. A. Isse, A. Gennaro and K. Matyjaszewski, *Macromolecules*, 2013, **46**, 8749-8772.
81. D. Konkolewicz, Y. Wang, P. Krys, M. Zhong, A. A. Isse, A. Gennaro and K. Matyjaszewski, *Polym. Chem.*, 2014, **5**, 4396-4417.

82. N. Bortolamei, A. A. Isse, A. J. D. Magenau, A. Gennaro and K. Matyjaszewski, *Angewandte Chemie International Edition*, 2011, **50**, 11391-11394.
83. D. Konkolewicz, K. Schröder, J. Buback, S. Bernhard and K. Matyjaszewski, *ACS Macro Letters*, 2012, **1**, 1219-1223.
84. X. Pan, C. Fang, M. Fantin, N. Malhotra, W. Y. So, L. A. Peteanu, A. A. Isse, A. Gennaro, P. Liu and K. Matyjaszewski, *Journal of the American Chemical Society*, 2016, **138**, 2411-2425.
85. X. Pan, M. A. Tasdelen, J. Laun, T. Junkers, Y. Yagci and K. Matyjaszewski, *Progress in Polymer Science*, 2016, **62**, 73-125.
86. Z. Wang, X. Pan, L. Li, M. Fantin, J. Yan, Z. Wang, Z. Wang, H. Xia and K. Matyjaszewski, *Macromolecules*, 2017, **50**, 7940-7948.
87. Z. Wang, X. Pan, J. Yan, S. Dadashi-Silab, G. Xie, J. Zhang, Z. Wang, H. Xia and K. Matyjaszewski, *ACS Macro Letters*, 2017, **6**, 546-549.
88. H. Mohapatra, M. Kleiman and A. P. Esser-Kahn, *Nature Chemistry*, 2017, **9**, 135-139.
89. N. V. Tsarevsky, T. Pintauer and K. Matyjaszewski, *Macromolecules*, 2004, **37**, 9768-9778.
90. A. Simakova, S. E. Averick, D. Konkolewicz and K. Matyjaszewski, *Macromolecules*, 2012, **45**, 6371-6379.
91. D. Konkolewicz, A. J. D. Magenau, S. E. Averick, A. Simakova, H. He and K. Matyjaszewski, *Macromolecules*, 2012, **45**, 4461-4468.
92. Z. Wang, M. Fantin, J. Sobieski, Z. Wang, J. Yan, J. Lee, T. Liu, S. Li, M. Olszewski, M. R. Bockstaller and K. Matyjaszewski, *Macromolecules*, 2019, **52**, 8713-8723.
93. M. N. Tchoul, M. Dalton, L.-S. Tan, H. Dong, C. M. Hui, K. Matyjaszewski and R. A. Vaia, *Polymer*, 2012, **53**, 79-86.
94. K. Min, H. Gao and K. Matyjaszewski, *Macromolecules*, 2007, **40**, 1789-1791.
95. C. M. R. Abreu, L. Fu, S. Carmali, A. C. Serra, K. Matyjaszewski and J. F. J. Coelho, *Polymer Chemistry*, 2017, **8**, 375-387.
96. Q. Wei, M. Sun, F. Lorandi, R. Yin, J. Yan, T. Liu, T. Kowalewski and K. Matyjaszewski, *Macromolecules*, 2021, **54**, 1631-1638.
97. M. Fantin, F. Lorandi, A. A. Isse and A. Gennaro, *Macromolecular Rapid Communications*, 2016, **37**, 1318-1322.
98. F. Lorandi, M. Fantin, A. A. Isse and A. Gennaro, *Polymer Chemistry*, 2016, **7**, 5357-5365.
99. A. Anastasaki, V. Nikolaou, Q. Zhang, J. Burns, S. R. Samanta, C. Waldron, A. J. Haddleton, R. McHale, D. Fox, V. Percec, P. Wilson and D. M. Haddleton, *Journal of the American Chemical Society*, 2014, **136**, 1141-1149.
100. E. H. Discekici, A. Anastasaki, R. Kaminker, J. Willenbacher, N. P. Truong, C. Fleischmann, B. Oschmann, D. J. Lunn, J. Read de Alaniz, T. P. Davis, C. M. Bates and C. J. Hawker, *Journal of the American Chemical Society*, 2017, **139**, 5939-5945.
101. S. Dadashi-Silab, I.-H. Lee, A. Anastasaki, F. Lorandi, B. Narupai, N. D. Dolinski, M. L. Allegrezza, M. Fantin, D. Konkolewicz, C. J. Hawker and K. Matyjaszewski, *Macromolecules*, 2020, **53**, 5280-5288.
102. S. Dadashi-Silab, F. Lorandi, M. J. DiTucci, M. Sun, G. Szczepaniak, T. Liu and K. Matyjaszewski, *Journal of the American Chemical Society*, 2021, DOI: 10.1021/jacs.1c04428.
103. W. Zhang, J. He, C. Lv, Q. Wang, X. Pang, K. Matyjaszewski and X. Pan, *Macromolecules*, 2020, **53**, 4678-4684.
104. N. A. Lynd and M. A. Hillmyer, *Macromolecules*, 2005, **38**, 8803-8810.
105. O. Terreau, L. Luo and A. Eisenberg, *Langmuir*, 2003, **19**, 5601-5607.
106. R. Whitfield, N. P. Truong and A. Anastasaki, *Angewandte Chemie International Edition*, 2021, **60**, 19383-19388.
107. D. T. Gentekos, L. N. Dupuis and B. P. Fors, *Journal of the American Chemical Society*, 2016, **138**, 1848-1851.
108. V. Kottisch, D. T. Gentekos and B. P. Fors, *ACS Macro Letters*, 2016, **5**, 796-800.
109. N. Corrigan, R. Manahan, Z. T. Lew, J. Yeow, J. Xu and C. Boyer, *Macromolecules*, 2018, **51**, 4553-4563.
110. M. H. Reis, T. P. Varner and F. A. Leibfarth, *Macromolecules*, 2019, **52**, 3551-3557.
111. J. Morsbach, A. H. E. Müller, E. Berger-Nicoletti and H. Frey, *Macromolecules*, 2016, **49**, 5043-5050.
112. X. Liu, C.-G. Wang and A. Goto, *Angewandte Chemie International Edition*, 2019, **58**, 5598-5603.
113. R. P. Quirk and B. Lee, *Polymer International*, 1992, **27**, 359-367.
114. T. Sarbu, K.-Y. Lin, J. Ell, D. J. Siegwart, J. Spanswick and K. Matyjaszewski, *Macromolecules*, 2004, **37**, 3120-3127.
115. J. Yan, T. Kristufek, M. Schmitt, Z. Wang, G. Xie, A. Dang, C. M. Hui, J. Pietrasik, M. R. Bockstaller and K. Matyjaszewski, *Macromolecules*, 2015, **48**, 8208-8218.
116. C.-G. Wang, A. M. L. Chong and A. Goto, *ACS Macro Letters*, 2021, **10**, 584-590.
117. V. Yadav, N. Hashmi, W. Ding, T.-H. Li, M. K. Mahanthappa, J. C. Conrad and M. L. Robertson, *Polymer Chemistry*, 2018, **9**, 4332-4342.
118. M. Rolland, N. P. Truong, R. Whitfield and A. Anastasaki, *ACS Macro Letters*, 2020, **9**, 459-463.
119. A. Plichta, M. Zhong, W. Li, A. M. Elsen and K. Matyjaszewski, *Macromolecular Chemistry and Physics*, 2012, **213**, 2659-2668.
120. Y. Wang and K. Matyjaszewski, *Macromolecular Rapid Communications*, 2020, **41**, 2000264.
121. C. Y. Lin, S. R. A. Marque, K. Matyjaszewski and M. L. Coote, *Macromolecules*, 2011, **44**, 7568-7583.
122. M. Lamson, M. Kopeć, H. Ding, M. Zhong and K. Matyjaszewski, *Journal of Polymer Science Part A: Polymer Chemistry*, 2016, **54**, 1961-1968.
123. T. Fukuda, *Journal of Polymer Science Part A: Polymer Chemistry*, 2004, **42**, 4743-4755.
124. R. Whitfield, K. Parkatzidis, M. Rolland, N. P. Truong and A. Anastasaki, *Angewandte Chemie International Edition*, 2019, **58**, 13323-13328.
125. M. Rolland, V. Lohmann, R. Whitfield, N. P. Truong and A. Anastasaki, *Journal of Polymer Science*, 2021, **n/a**.
126. M. Szwarc, M. Levy and R. Milkovich, *Journal of the American Chemical Society*, 1956, **78**, 2656-2657.
127. F. S. Bates and G. H. Fredrickson, *Annual Review of Physical Chemistry*, 1990, **41**, 525-557.
128. L. Leibler and H. Benoit, *Polymer*, 1981, **22**, 195-201.
129. D. M. Cooke and A.-C. Shi, *Macromolecules*, 2006, **39**, 6661-6671.
130. S. W. Sides and G. H. Fredrickson, *The Journal of Chemical Physics*, 2004, **121**, 4974-4986.
131. J. Listak, X. Jia, A. Plichta, M. Zhong, K. Matyjaszewski and M. R. Bockstaller, *Journal of Polymer Science Part B: Polymer Physics*, 2012, **50**, 106-116.
132. S. T. Milner, T. A. Witten and M. E. Cates, *Macromolecules*, 1989, **22**, 853-861.
133. T. B. Martin, P. M. Dodd and A. Jayaraman, *Physical Review Letters*, 2013, **110**, 018301.
134. W. M. de Vos, F. A. M. Leermakers, A. de Keizer, J. M. Kleijn and M. A. Cohen Stuart, *Macromolecules*, 2009, **42**, 5881-5891.

135. A. Muñoz-Bonilla, A. M. van Herk and J. P. A. Heuts, *Macromolecules*, 2010, **43**, 2721-2731.
136. Y. Li, T. M. Krentz, L. Wang, B. C. Benicewicz and L. S. Schadler, *ACS Applied Materials & Interfaces*, 2014, **6**, 6005-6021.
137. S. Christau, J. Genzer and R. von Klitzing, *Zeitschrift für Physikalische Chemie*, 2015, **229**, 1089-1117.
138. P. Chmielarz, J. Yan, P. Krys, Y. Wang, Z. Wang, M. R. Bockstaller and K. Matyjaszewski, *Macromolecules*, 2017, **50**, 4151-4159.
139. W. Yan, S. Dadashi-Silab, K. Matyjaszewski, N. D. Spencer and E. M. Benetti, *Macromolecules*, 2020, **53**, 2801-2810.
140. Z. Wang, J. Yan, T. Liu, Q. Wei, S. Li, M. Olszewski, J. Wu, J. Sobieski, M. Fantin, M. R. Bockstaller and K. Matyjaszewski, *ACS Macro Letters*, 2019, **8**, 859-864.
141. Z. Wang, T. Liu, K. C. Lin, S. Li, J. Yan, M. Olszewski, J. Sobieski, J. Pietrasik, M. R. Bockstaller and K. Matyjaszewski, *Journal of Inorganic and Organometallic Polymers and Materials*, 2020, **30**, 174-181.
142. D. T. Gentekos, R. J. Sifri and B. P. Fors, *Nature Reviews Materials*, 2019, **4**, 761-774.
143. X. Ye and T. Sridhar, *Macromolecules*, 2005, **38**, 3442-3449.
144. M. Nadgorny, D. T. Gentekos, Z. Xiao, S. P. Singleton, B. P. Fors and L. A. Connal, *Macromolecular Rapid Communications*, 2017, **38**, 1700352.
145. R. A. Register, *Nature*, 2012, **483**, 167-168.
146. J. P. Koski and A. L. Frischknecht, *ACS Nano*, 2018, **12**, 1664-1672.
147. M. Elsabahy and K. L. Wooley, *Journal of Polymer Science Part A: Polymer Chemistry*, 2012, **50**, 1869-1880.
148. V. Goel, J. Pietrasik, R. Poling-Skutvik, A. Jackson, K. Matyjaszewski and R. Krishnamoorti, *Polymer*, 2018, **159**, 138-145.
149. Y. Li, P. Tao, A. Viswanath, B. C. Benicewicz and L. S. Schadler, *Langmuir*, 2013, **29**, 1211-1220.
150. Z. Wang, J. Lee, Z. Wang, Y. Zhao, J. Yan, Y. Lin, S. Li, T. Liu, M. Olszewski, J. Pietrasik, M. R. Bockstaller and K. Matyjaszewski, *ACS Macro Letters*, 2020, **9**, 806-812.
151. S. L. Baker, B. Kaupbayeva, S. Lathwal, S. R. Das, A. J. Russell and K. Matyjaszewski, *Biomacromolecules*, 2019, **20**, 4272-4298.
152. D. T. Gentekos, J. Jia, E. S. Tirado, K. P. Barteau, D.-M. Smilgies, R. A. DiStasio and B. P. Fors, *Journal of the American Chemical Society*, 2018, **140**, 4639-4648.